Electronic Supplementary Material (ESI) for RSC Advances.

Table 1 (Supplemental Data): Characterization via GC/MS analysis of end products from catalytic ketonization of model mixtures and water extracted fast pyrolysis oil using reduced red mud.

Reactants	Conditions W/F (h), T°C	Primary Products	GC/MS pKA[a], Match, Prob.%	Trace Products	GC/MS pKA[a], Match, Prob.%
Acetic Acid	2.3, 350°C	Acetone	0.6,944, 87	None	
Formic Acid	2.3, 350°C	None		Methanol	[b],965,76
				Acetic Acid	0.04,973,97
				Acetone	0.03,954,89
Acetol (2HP)	2.3, 350°C	Acetic Acid	0.34,958, 96	Acetaldehyde	0.035,863,56.2
		Acetone	0.62,942, 87	2,3-Butanedione	[b],862,74
		2-Butanone	0.09,923, 76	2,3-Pentadione	0.08,831,75
				2,5-Hexandione	0.04,899,74
				Propanoic Acid	0.27[c],851,75
				3-methyl cyclopentanone	0.10,904,35
				2-Cyclopenten-1-one, 2-methyl-	0.13,909,85
				2-Cyclopenten-1-one, 3-methyl-	0.18,864,61
Levoglucosan	2.3, 350°C	Acetic Acid	0.80,958,98	Acetaldehyde	0.03,877,77
		Formic Acid	HPLC	Acetone	0.08,892,72
		Acetol	0.13,895,85	2,3-Butanedione	0.03,957,82
				2,3-pentanedione	0.02,830,76
				2-Butanone	0.03,920,75
				Cyclopentanone	0.09,888,28
				2-Cyclopenten-1-one, 2-methyl-	0.06,944,65
				Furfural	0.06,899,44
				Levoglucosenone	0.02,863,88
AA, FA, 2HP	6, 400°C	Acetone	0.76,976, 92	Acetaldehyde	0.01,812, 46
		2-Butanone	0.53,943, 83	2-Butanone, 3-methyl-	0.09,891, 69
				2-Pentanone	0.09,905, 77
				3-Pentanone	0.12,937, 83
				2-Pentanone, 3-methyl-	0.05,856, 76
				3-Hexanone	0.11,837, 75
				Cyclopentanone	0.02,812, 39
				2-Cyclopenten-1-one, 2-methyl-	0.13,889, 77
				2-Cyclopenten-1-one, 3,4-dimethyl	0.03,862, 40

[a]ratio of component peak area to internal standard (hexanol, 2 g/L) in total ion mode; [b]present, but too small to integrate; [c]broad, poorly resolved peak

Table 4: Continued

Reactants	Conditions W/F (h), T°C	Primary Products	GC/MS pKA, Match, Prob.%	Trace Products	GC/MS pKA, Match, Prob.%
WE-FPO	4.2, 400°C	Acetone	1.3,944, 86	Methanol	0.67,878, 64
		2-Butanone	0.68,920, 77	Ethanol	0.07,894, 87
				2-Butanone, 3-methyl-	0.02,880, 51
				2-Pentanone	0.15,912, 80
				Cyclopentanone	0.19,900, 64
				2-Cyclopenten-1-one, 2-methyl-	0.42,936, 87
H_2 Effect				2-Cyclopenten-1-one, 3,4-dimethyl	0.16,917, 56
Acetol	2.8, 300°C, 600 psig	Acetic Acid	0.27,960, 96	Acetaldehyde	0.07,851,56
		Acetone	0.10,894, 66	2,3-Pentanedione	0.03,842,54
				2-Cyclopenten-1-one	0.25, 878,72
				5-Hydroxy-4-octanone	0.04,771,13
Acetol	2.8, 300°C, 600 psig, **H_2**	**Methanol**	0.14,921,75	Cyclopentanone	0.06,877,47
		Acetic Acid	0.15,944,95	Cyclopentanone, 2-methyl-	0.10,863,21
		Acetone	0.10,913,76	5-Hydroxy-4-octanone	0.20,780,14
Formic	2.8, 300°C, 600 psig	Acetic Acid	2.4,943,96	None	
		Acetone	0.08,880,80		
Formic	2.8, 300°C, 600 psig, **H_2**	**Methanol**	1.24,930, 91	Acetone	0.02,850,66
Levoglucosan	2.8, 300°C, 600 psig	Acetone	0.21,923, 81	Acetaldehyde	0.08,881, 45
		Acetic Acid	0.12,912, 92	Hydroxyacetic acid	0.03,829, 38
		Acetol	0.14,840, 73	2,3-Butanedione	0.06,873, 76
				2-Butanone	0.1,896, 45
				2,3-Pentanedione	0.04,870, 67
				Cyclopentanone	0.05,847, 41
				2-Cyclopenten-1-one	0.13,861, 67
				2-Cyclopenten-1-one, 2-methyl-	0.09,890, 87

Table 4: Continued

Reactants	Conditions W/F (h), T°C	Primary Products	GC/MS pKA, Match, Prob.%	Trace Products	GC/MS pKA, Match, Prob.%
Levoglucosan	2.8, 300°C, 600 psig, $\mathbf{H_2}$	Acetol	0.24,906, 82	2-Butanone	0.04,810, 19
		Methanol	0.09,905, 48	Cyclopentanone	0.06,864, 64
		Acetone	0.07,830, 58		

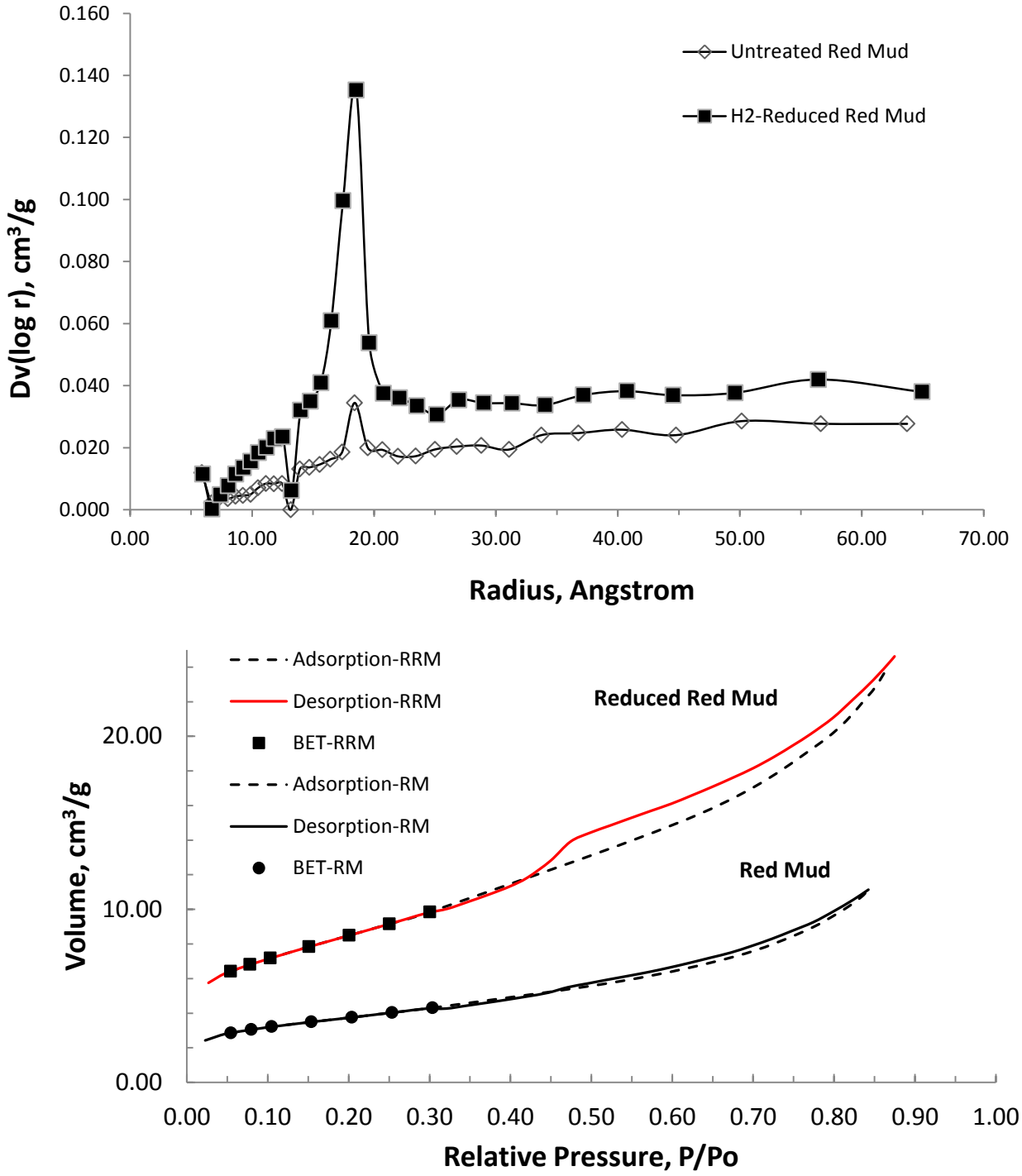

Figure 1(Supplemental Data): Pore size distribution (BJH analysis) and isotherms for red mud (RM) and H_2 reduced red mud (RRM) [top] and isotherms (bottom). BET indicates points used in surface area calculation.

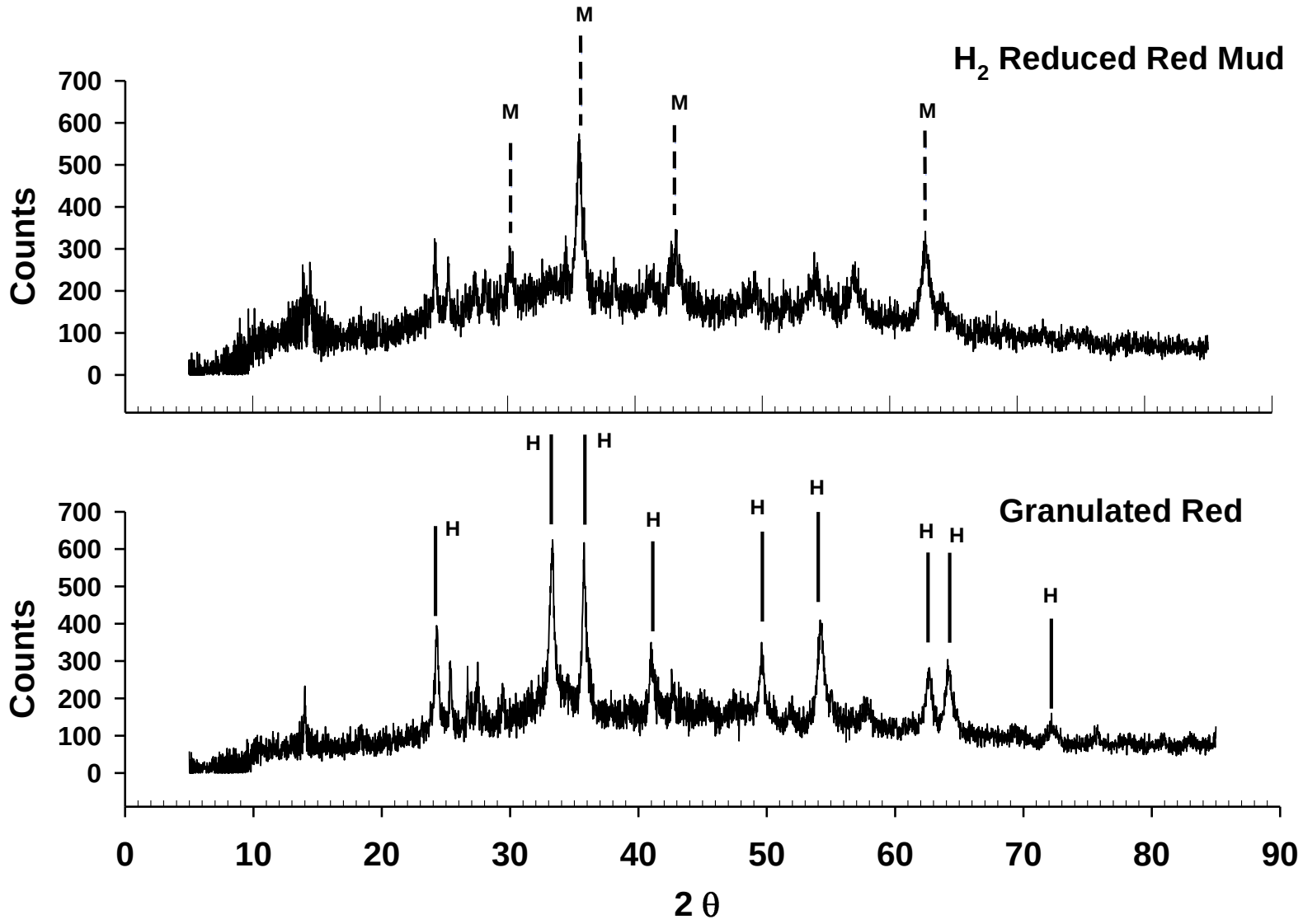

Figure 2 (SD): XRD analysis of red mud, and H_2 reduced red mud (RRM) catalyst samples. H and M indicates hematite and magnetite signals, respectively.

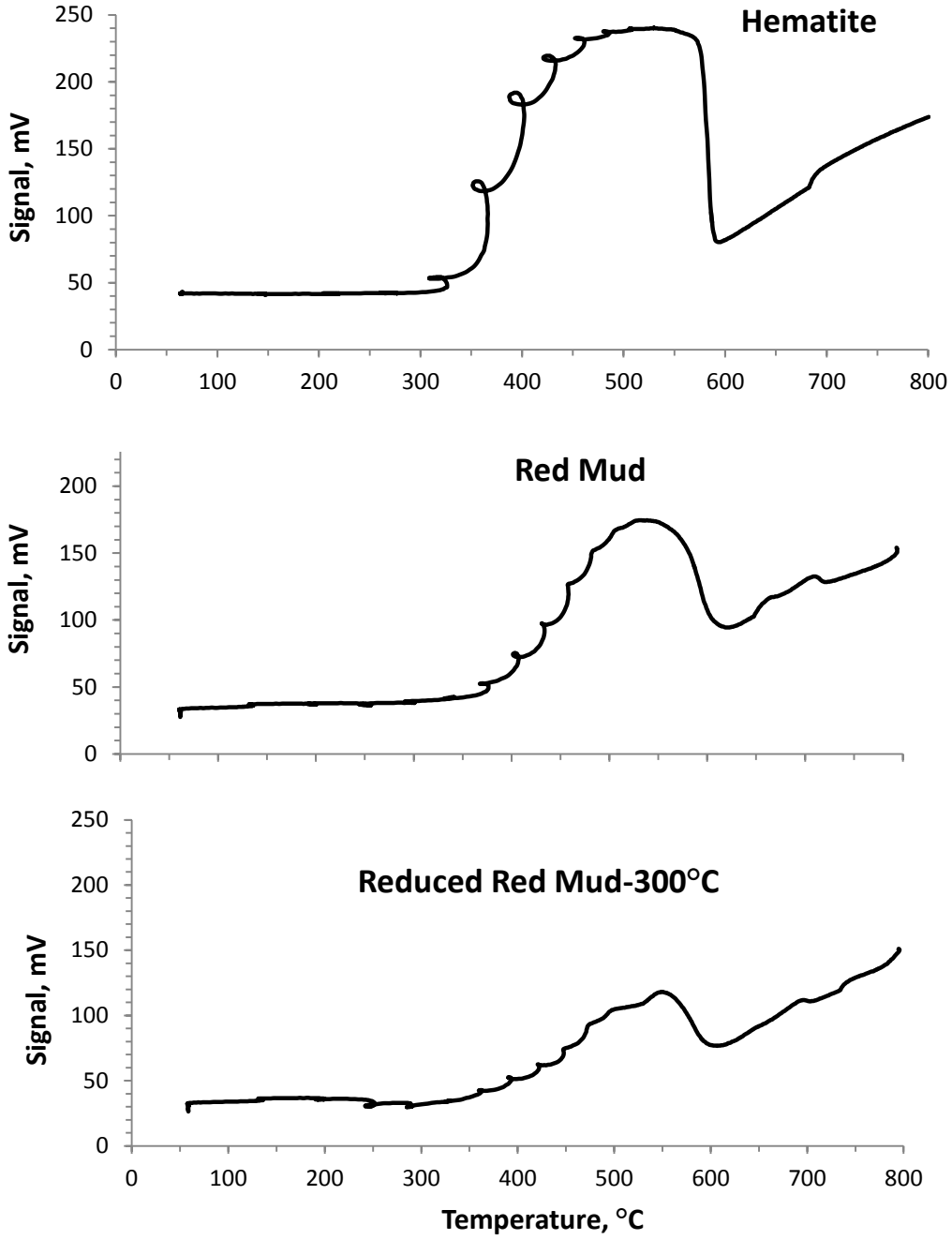

Figure 3 (SD): Temperature programmed reduction of hematite, red mud, and red mud reduced with H_2 at 300°C. The small loops in signal response from 100 to 500°C are due to a non-linear heating profile.

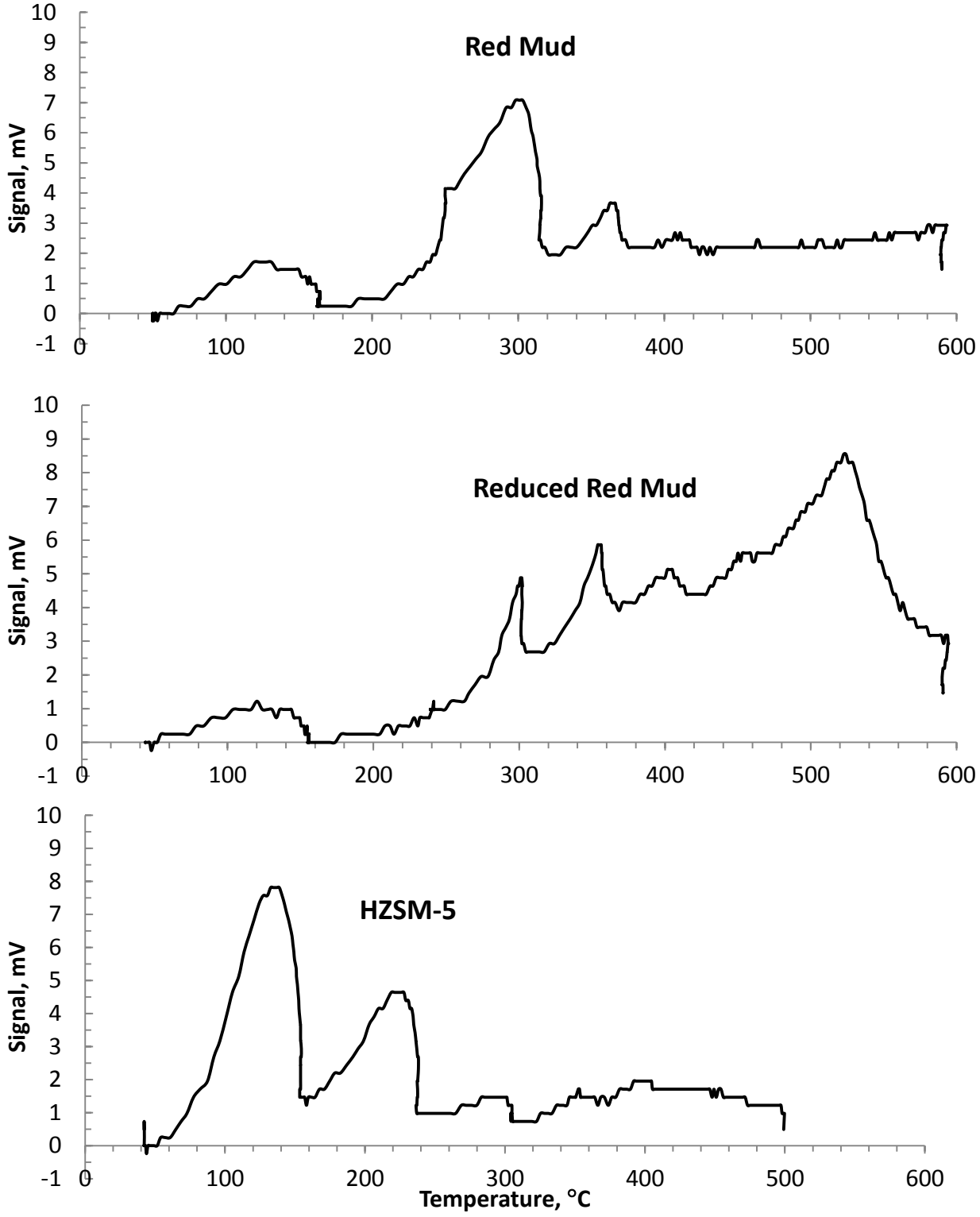

Figure 4 (SD): Ammonia temperature programmed desorption of red mud (top) and reduced red mud (middle), compared with the acidic zeolite, H-ZSM5 (bottom).

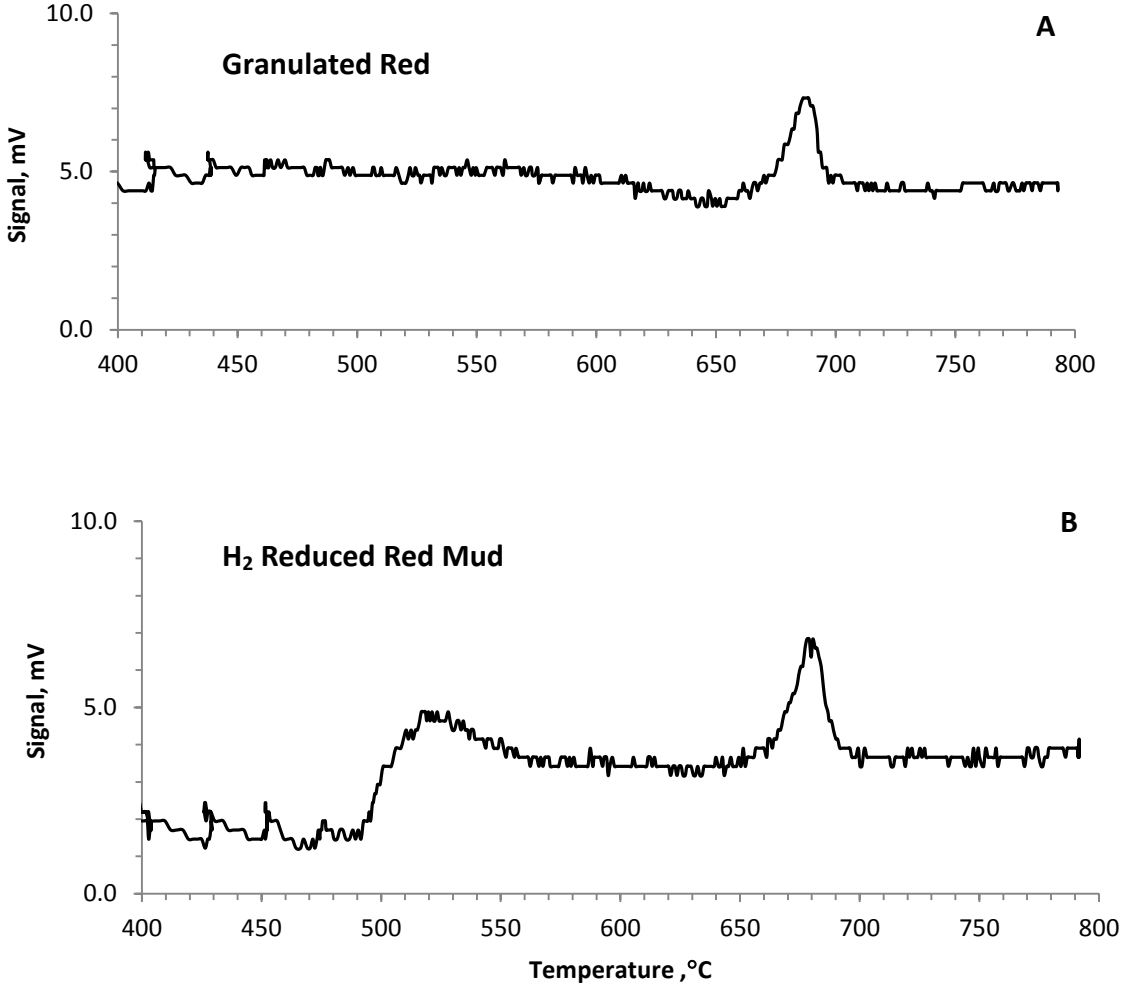

Figure 5 (SD): Carbon dioxide temperature programmed desorption of red mud (A) and reduced red mud (B) with a blank run subtracted [CO_2 was not pre-adsorbed for blank].

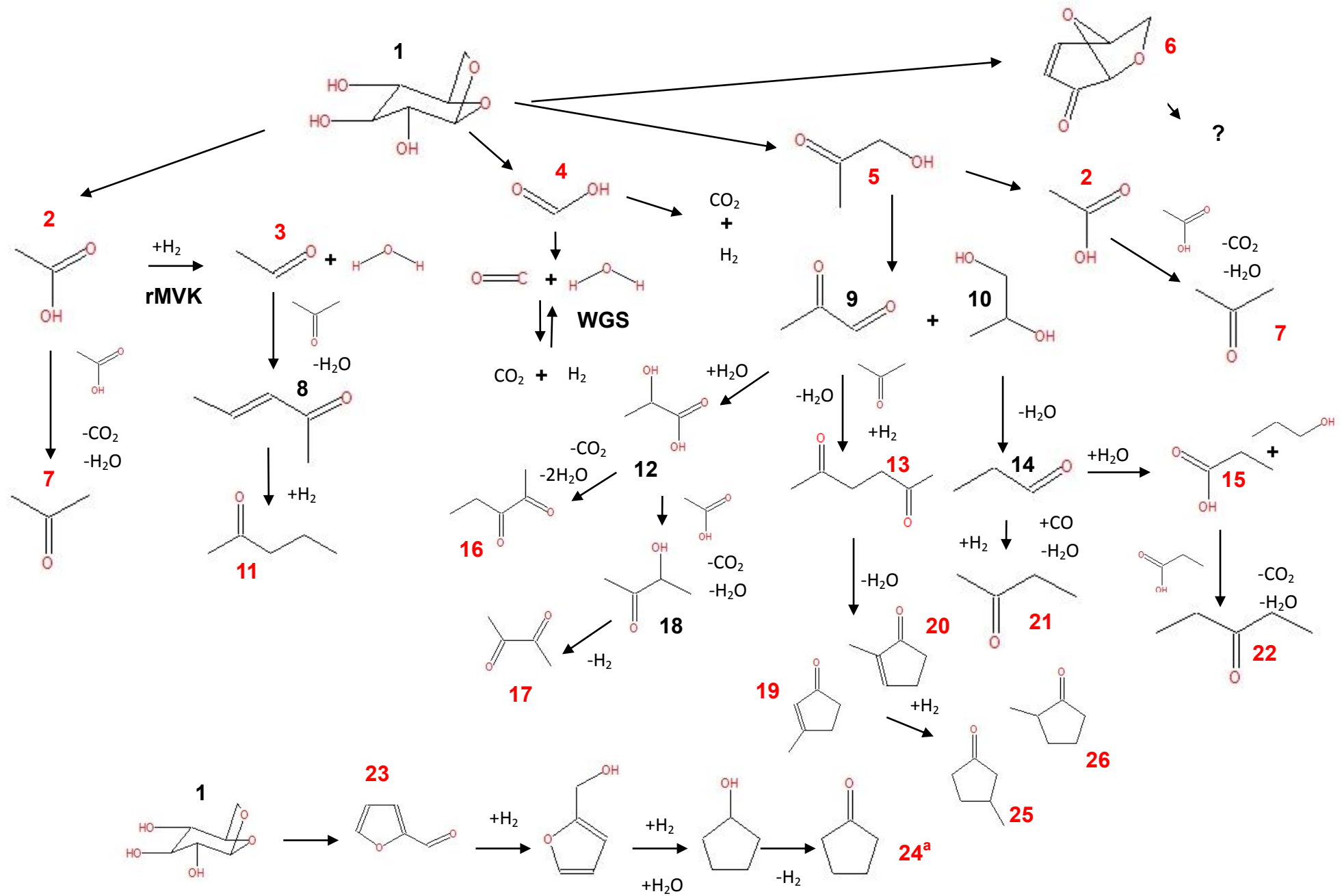

Figure 6SD: Potential ketonization, dehydration, condensation, and hydrogenation pathways leading to products from levoglucosan (1), acetic acid (2), formic acid (4), and acetol (5). Compounds numbered in red were identified by GC/MS, rMVK indicates reverse Mars van Krevelen mechanism, and WGS indicates water gas shift reaction. Intermediates and products include levoglucosenone (6), acetaldehyde (3), pyruvaldehyde (9), propylene glycol (10), acetone (7), 3-penten-2-one (8), 2-pentanone (11), lactic acid (12), 2,5-hexanedione (13), propanal (14), propanoic acid (15), 2,3-pentanedione (16), 2,3-butanedione (17), 3-hydroxy-2-butanone (18), 3-methyl-2-cyclopenten-1-one (19), 2-methyl-2-cyclopenten-1-one (20), 2-butanone (21), 3-pentanone (22), furfural (23), cyclopentanone (24), 2-methylcyclopentanone (26), and 3-methylcyclopentanone (25). References: S. H. Hakim, B. H. Shanks, J. A. Dumesic, *Applied Catalysis B: Environmental*, 2013, **142–143**, 368– 376; P. Mäki-Arvela, I. L. Simakova, T. Salmi, D. Y. Murzin, *Chem. Rev.*, 2014, **114**, 1909−1971. [a] M. Hronec, K. Fulajtarova, T. Liptaj. *Applied Catalysis A: General*, 2012, 437-438, 104-111.

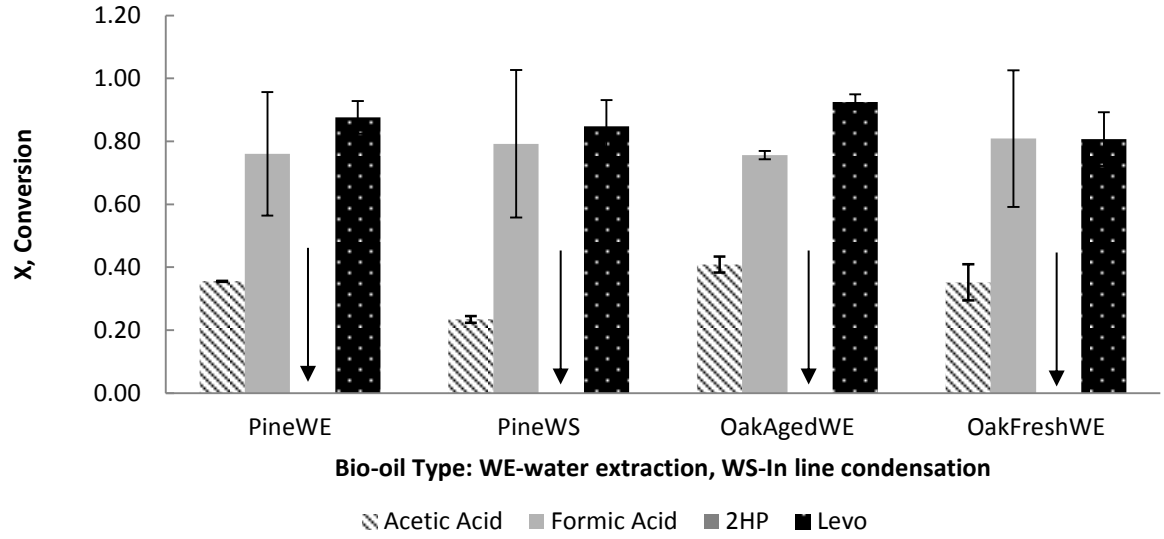

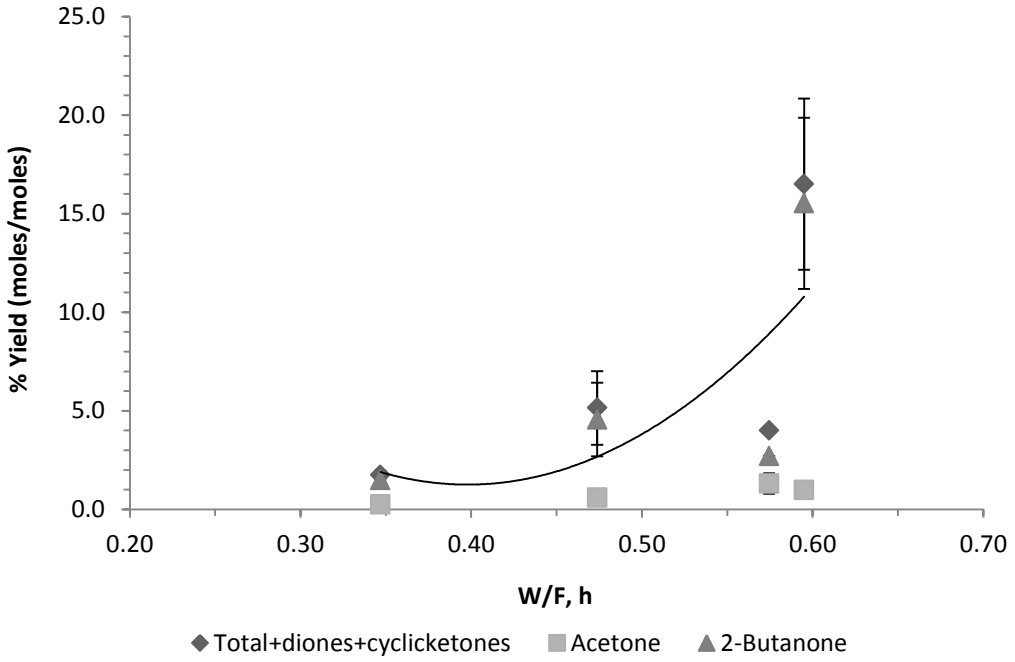

Figure 7 (SD): Catalytic ketonization of water extracted fast pyrolysis oil using reduced red mud at 350°C and 1 atm (W/F = 1/WHSV or weight hourly space velocity, g-measurable feed/g-cat/h). Note, the concentrations of diketones and cyclic ketones were estimated using single point standards and GC/MS analysis with an external standard. 2HP is acetol and Levo is levoglucosan. Arrows indicate that the net conversion of 2HP did not occur.

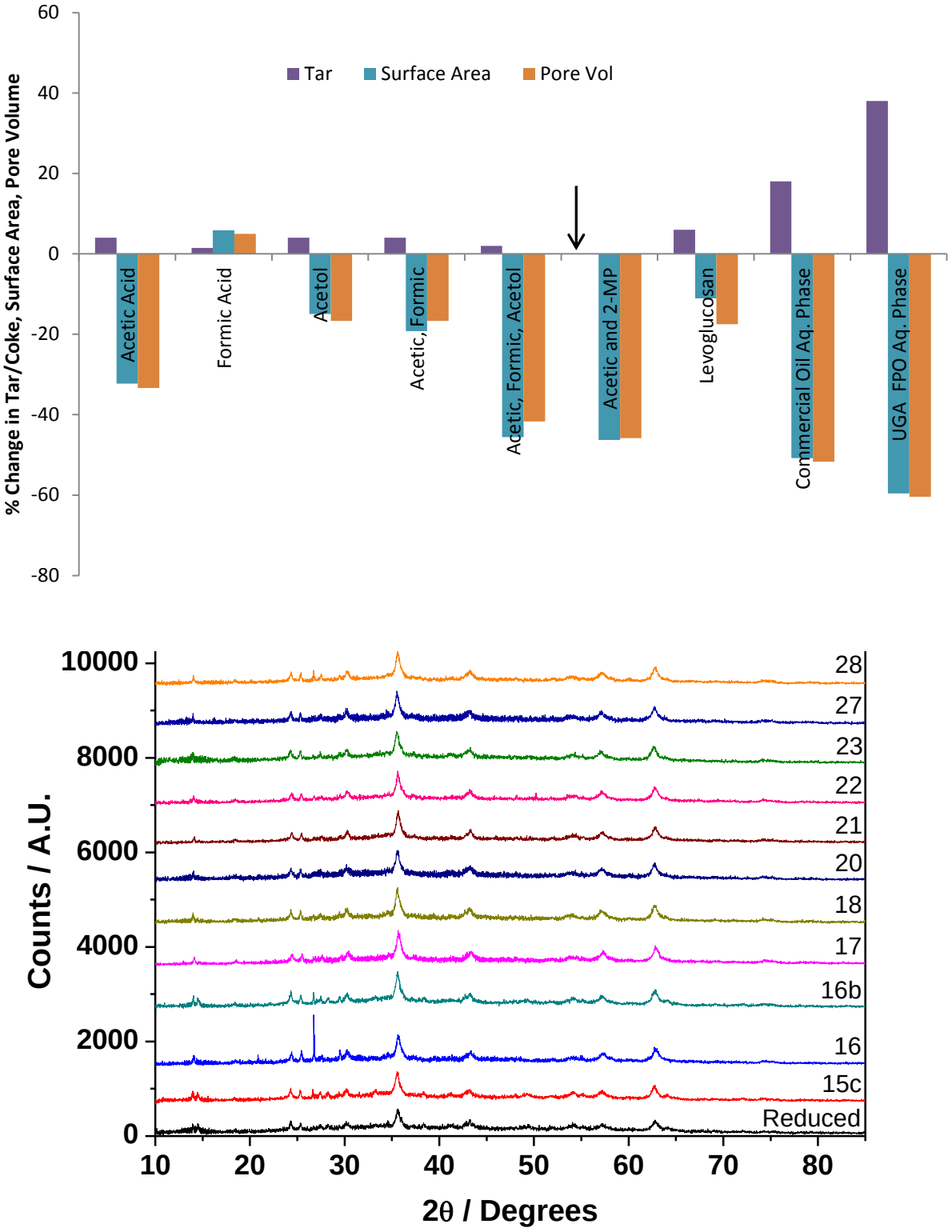

Figure 8 (SD): Change in catalyst surface area, pore volume, tar, and crystal structure (XRD) upon reaction with individual compounds (28, levoglucosan; 17, acetol; 16B, formic; 15C, acetic), mixtures (18,AA-FA; 16, AA-FA-Acetol; 20,AA-2MP), and water extracted FPO (23&27,CO; 21&22,UGA WE-oil), at 350°C and 1 atm. The arrow indicates no change in tar after reaction with acetic and 2-methoxy phenol (or 2-MP). AA is acetic acid, FA formic acid, acetol is 1-hydroxy-2-propanone, CO is water extracted commercial oil.

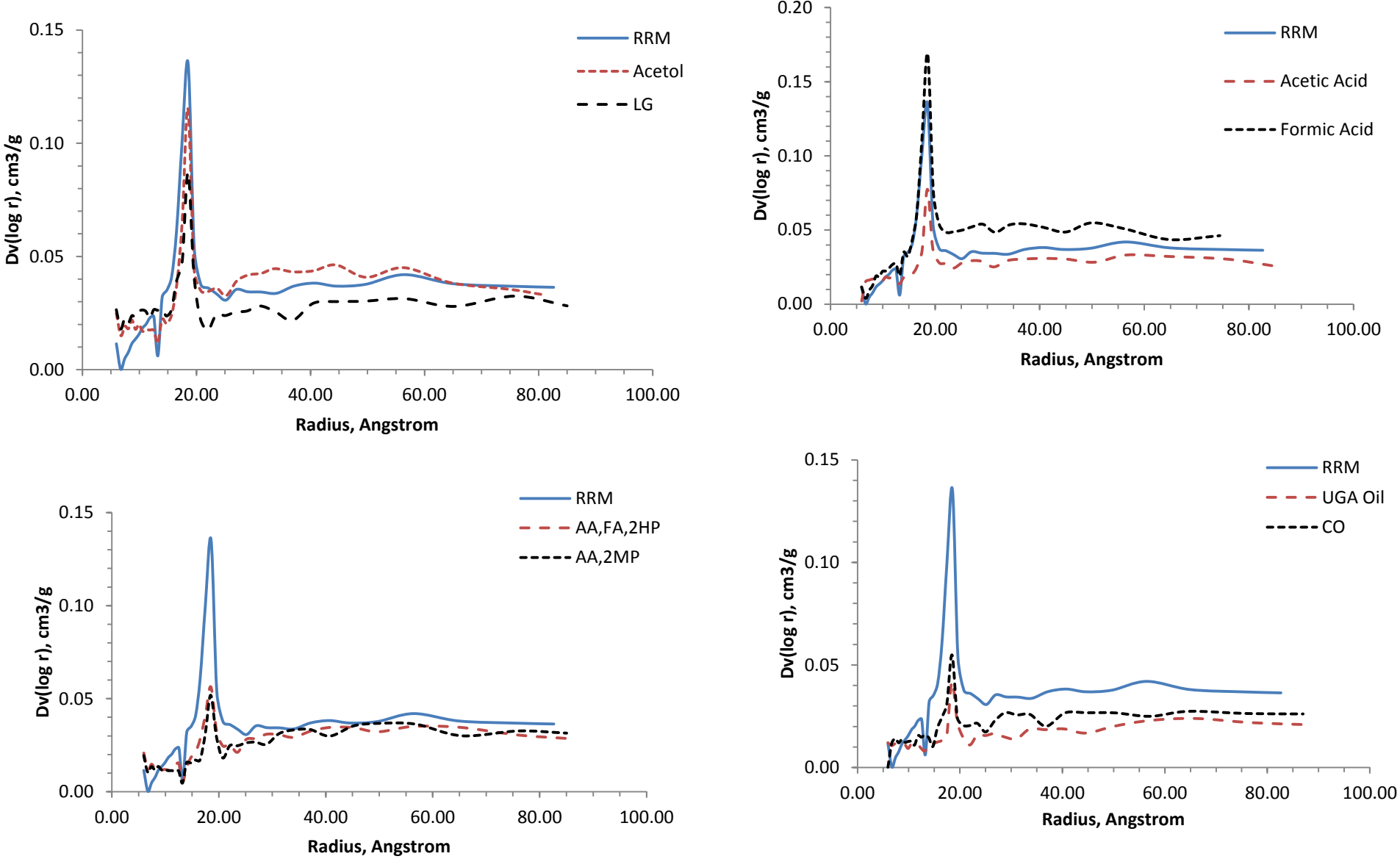

Figure 9 (SD): Effect of reaction on pore size distribution measured from the N_2 desorption curve during BET analysis of the catalyst surface properties. LG is levoglucosan, acetol or 2HP is 1-hydroxy-2-propanone, 2MP is 2-methoxy phenol, AA is acetic acid, CO is commercial fast pyrolysis oil.

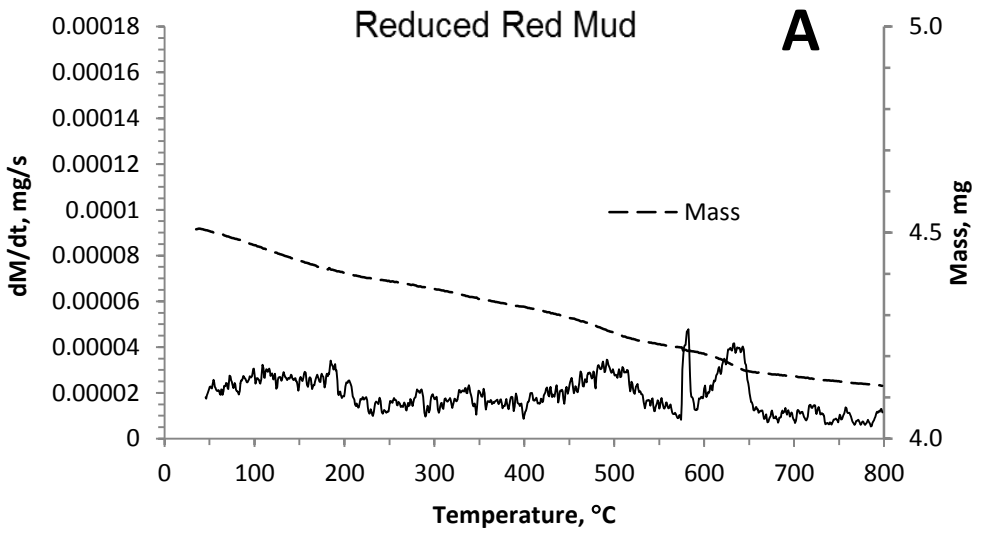
Reduced Red Mud
A
dM/dt, mg/s
Mass, mg
Mass
Temperature, °C
0.00018
0.00016
0.00014
0.00012
0.0001
0.00008
0.00006
0.00004
0.00002
0
5.0
4.5
4.0
0
100
200
300
400
500
600
700
800

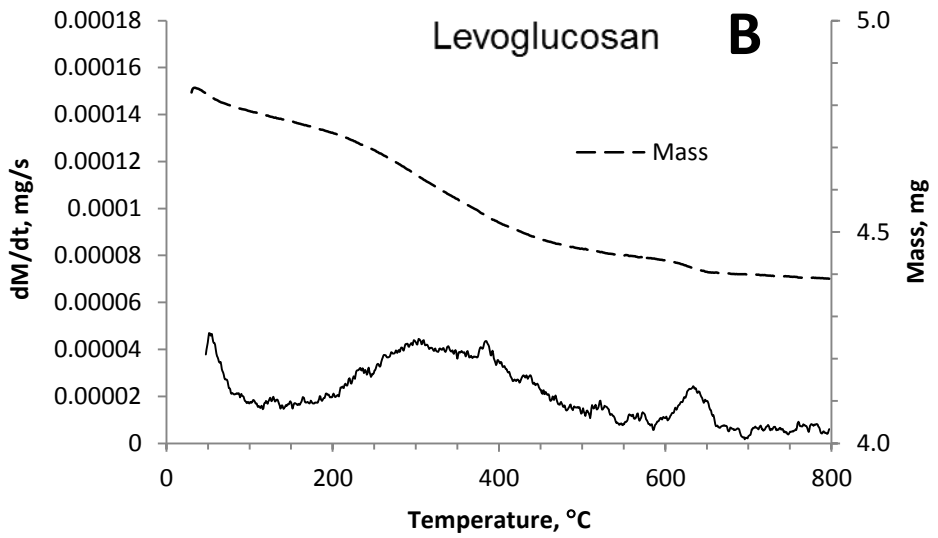
Levoglucosan
B
dM/dt, mg/s
Mass, mg
Mass
Temperature, °C
0.00018
0.00016
0.00014
0.00012
0.0001
0.00008
0.00006
0.00004
0.00002
0
5.0
4.5
4.0
0
200
400
600
800

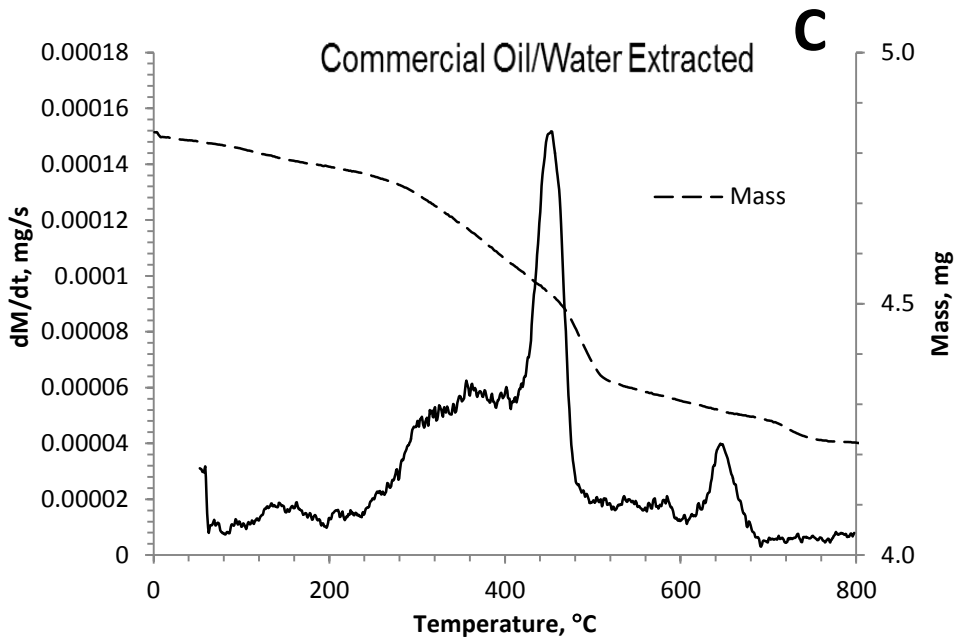
Commercial Oil/Water Extracted
C
dM/dt, mg/s
Mass, mg
Mass
Temperature, °C
0.00018
0.00016
0.00014
0.00012
0.0001
0.00008
0.00006
0.00004
0.00002
0
5.0
4.5
4.0
0
200
400
600
800

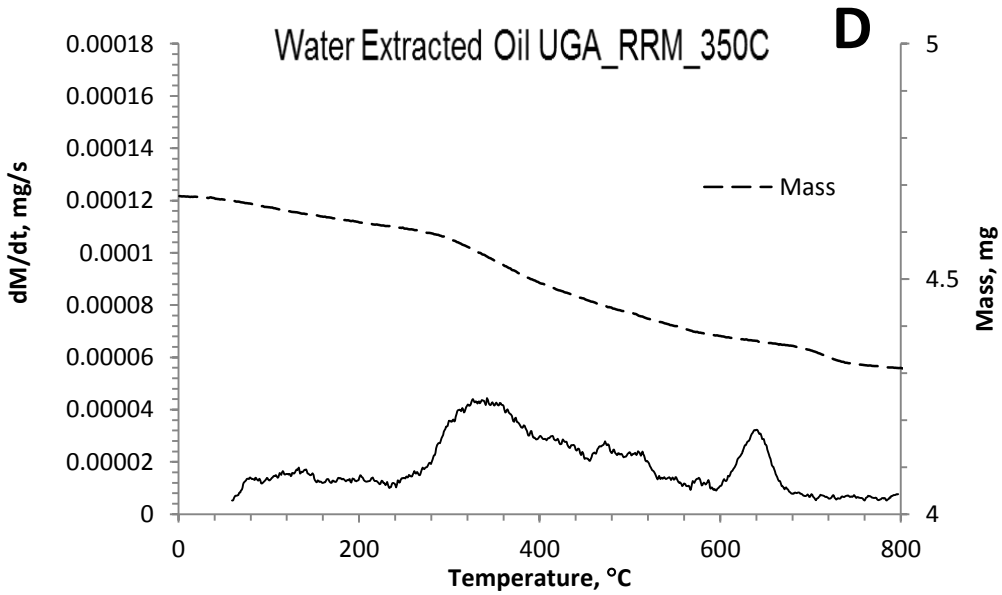
Water Extracted Oil UGA_RRM_350C
D
dM/dt, mg/s
Mass, mg
Mass
Temperature, °C
0.00018
0.00016
0.00014
0.00012
0.0001
0.00008
0.00006
0.00004
0.00002
0
5
4.5
4
0
200
400
600
800

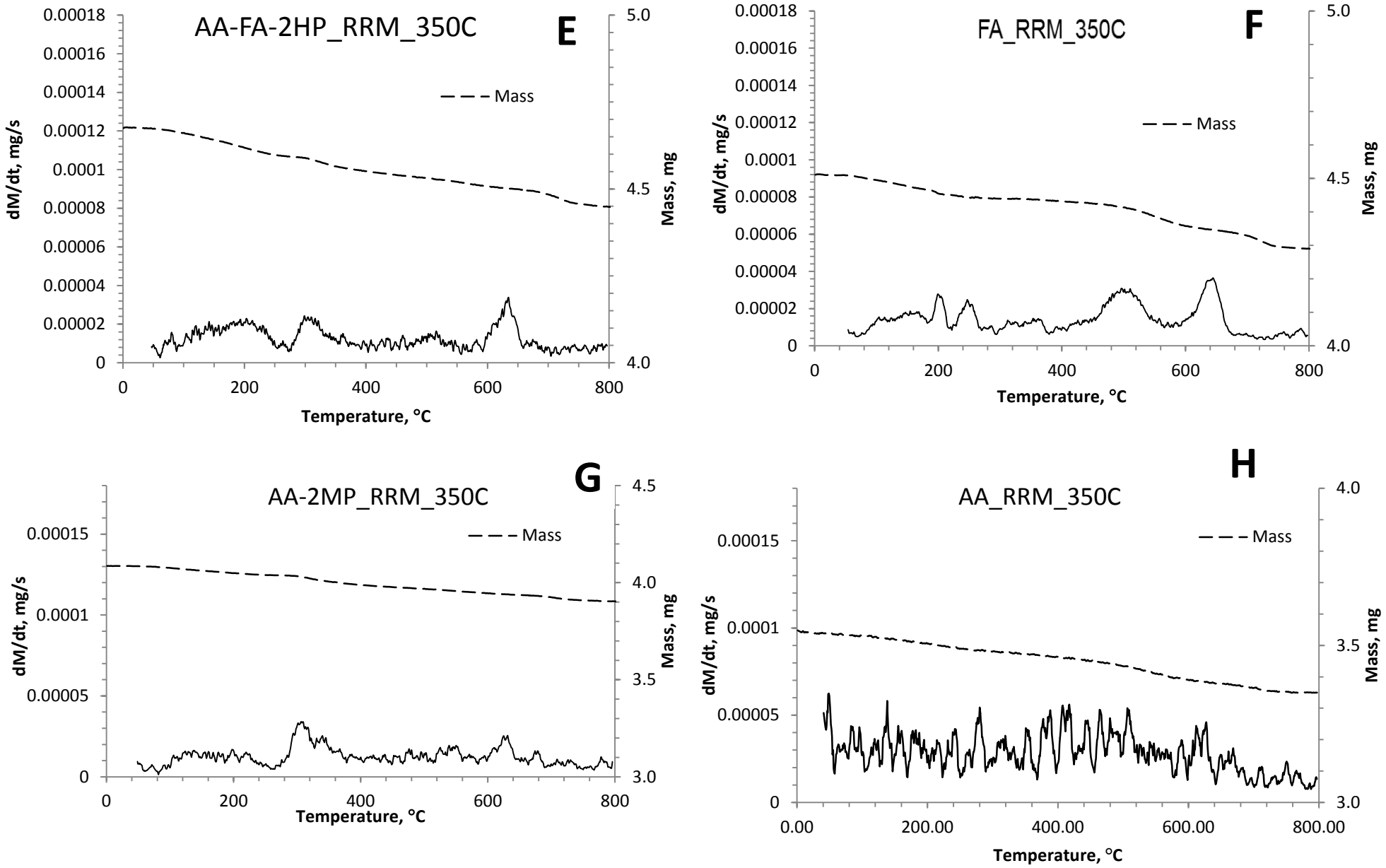

Figure 10 (SD): Oxidative TGA analysis of spent catalyst (300°C H_2 reduced red mud, A) after catalytic ketonization of levoglucosan (B), commercial oil (C), UGA oil (D), acetic acid with 2-methoxy phenol (E), formic acid (F), and a mixture of acetic acid, formic acid, and 1-hydroxy-2-propanone (G), and acetic acid alone (H). Note: The catalysts were solvent washed and dried before TGA analysis and the first derivative of the mass loss data is presented as a positive value.